Proceedings of Ninth World Conference on Earthquake Engineering
August 2-9, 1988, Tokyo-Kyoto, JAPAN (Vol.VI)

10-1-25

DYNAMIC FAILURE TESTS ON MODEL EMBANKMENTS AND NUMERICAL SIMULATIONS OF THEM

Hiroyuki WATANABE[1] and Atsushi SAOTOME[2]

[1]Department of Construction Engineering, Saitama University, Urawa-shi, Saitama, Japan
[2]Department of Civil Engineering Design, Electric Power Development Co., Chuoh-ku, Tokyo, Japan

SUMMARY

Presented in this paper are the dynamic failure patterns of model embankments of moistured sand obtained throughout the experiments carried on a shaking table and those simulations. From the experiments it is found that dynamic failure shows a frequency dependency and differs remarkably from static one observed in tilting tests. Both equivalent linear dynamic analysis and non-linear one simulate fairly well above results clarifying those mechanism to some extent.

INTRODUCTION

In the assessment of seismic stability of soil structures, only conventional method such as so-called seismic coefficient method is officially approved and dynamic analysis is regarded as supplemental method in Japan. In order to authorize dynamic analysis, it is necessary for the engineers to understand clearly the correlation of both methods. Some parts of it have been successfully understood. For an example, the factor of safety in a potential sliding surface obtained from dynamic analysis at arbitrary instant does agree well with the one calculated with the conventional method against the seismic coefficient equivalent to the inertia force estimated in dynamic analysis at same instant(Ref.1). The correlation of failure patterns defined by both methods, however, remains unknown. In elucidating it, a mechanism resulting in each failure pattern must be clarified. Some characteristics of failure supposed in the conventional method were discussed by the authors(Ref.2) on the basis of experiments and a non-linear analysis where model slopes of same sand as in this paper were failured statically by horizontal and vertical gravity forces generated with tilting them. In this paper presented are dynamic failure patterns, those simulations and comparison of dynamic failure with static one quoted from the reference.

DYNAMIC FAILURE TESTS ON MODEL EMBANKMENTS

Methods A diluvial sand borrowed from a power station was used for the models, which is classified as SC according to Japanese Unified Soil Classification System. Its grain size accumulation curve is shown in Fig.1. All models were constructed by means of compaction in a testing box of steel on a shaking table and were 1(m) in the height, 0.7(m) in the width of flat top, 1:2.0 in the slopes of both sides and 4.5(m) in the length of axial direction. Index properties of the sand are 2.65 in specific gravity, 16.2(%) in optimum water content and 1.715(gr/cm^3) in

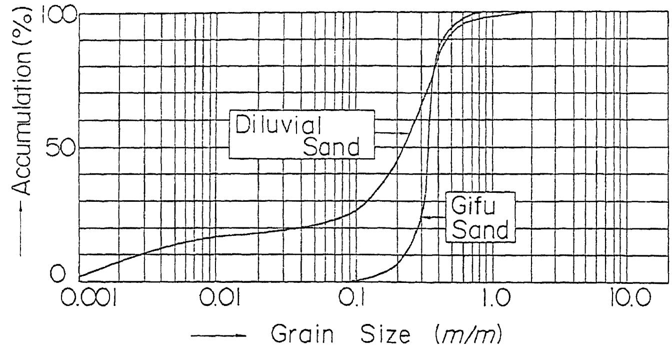

Fig. 1 Grain Size Accumulation Curves of Tested Sands

maximum dry density. Throughout total series of the experiments including the static tests mentioned above, void ratio, water content, density and shear wave velocity of all models were 1.1, 14(%), 1.45(gr/cm^3) and 67(m/s) on the average respectively. In every model 18 acceleration meters in horizontal direction were arranged at the lattice points in half side of cross section as shown in Fig.5 and 4 ones in the vertical at those points on the slope. In order to detect occurring and the position of sliding, 3 displacement meters of thin phosphoric copper plate were embedded in vertical direction as shown in Fig.2. On the upper part of each plate 5 paper strain gauges were pasted at intervals of 5(cm) so as to search its deflection due to sliding in a model.

Resonant curves were made first on every model under the intensity of base acceleration of 25, 50, 75 and 100(gal). Measured resonant frequencies changed from about 20 to 15(Hz) as base acceleration increased. After these tests every model was excited with the sinusoidal base motion of constant frequency and of stepwise increasing amplitude untill failure occurred. Five sorts of frequency in all including 15(Hz) were adopted to the tests and two models were failured with every frequency. When failure starts strain gauges indicate it as shown in Fig.2.

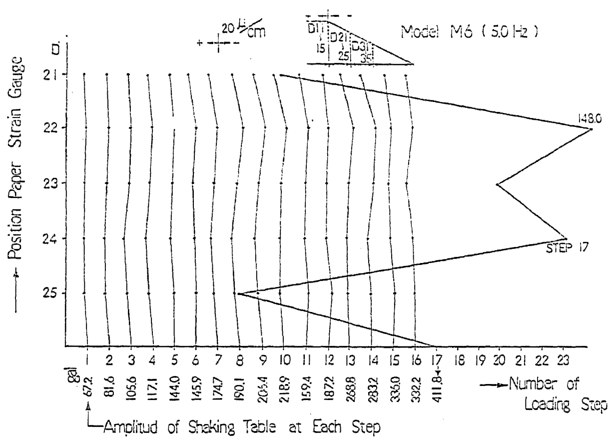

Fig. 2 Behavior of Strain on Displacement Meter

Results Fig.3 shows a relationship between measured accelerations at the instant of starting of failure and frequency of base motion. It may be seen that accel-

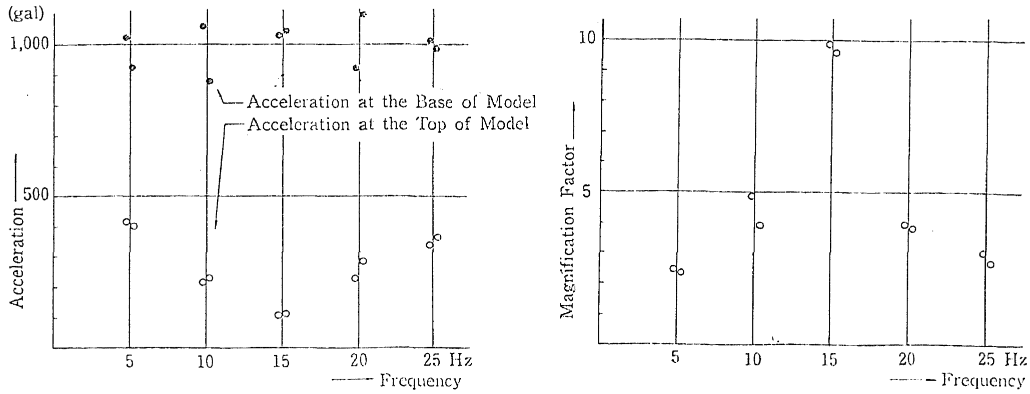

Fig. 3 Relationship between Acceleration at Failure and Frequency of Base Motion

eration at top of model on begining of failure seems to be kept constant at near around 1000(gal) as frequency of base motion changes from 5 to 25(Hz). Fig.4 shows some typical views of failured models and Fig.5 shows contours of amplification of maximum response acceleration at failure in the cross section of model.

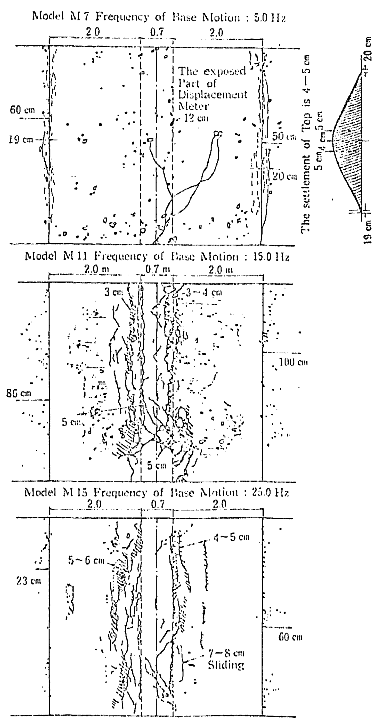

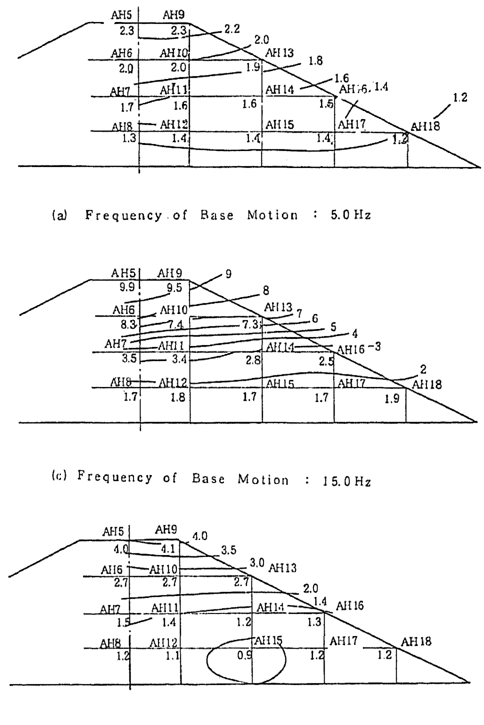

Fig. 4 Typical Views of Failure of Model Embankments

Fig. 5 Contours of Magnification of Response Acceleration on Begining of Failure

Failure patterns are summarized as follows.

(1) In all cases failured zone concentrated around crest.

(2) In the failure with frequency of 5(Hz), top part of 4~5(cm) in thickness was broken down in a moment when base acceleration attained to 400(gal), however, there was no damage in the lower part including slope surface.
(3) In the case of 15(Hz), that is, in resonance a crack parallel to the axis appeared at the portion of 20~30(cm) below crest on each side slope surface, then similar cracks increased one after another towards crest resulting in lots of falling of tortoise-shaped soil blocks after cracks reached to crest. If excitation was continued, the amount of falling would increased and the shape of crest would become similar to the one in the case of 5(Hz).
(4) In the case of 25(Hz), a crack parallel to the axis appeared at the lower part of about a half height on each surface, then similar cracks grew towards crest resulting in falling of smaller sized soil blocks around crest.

As mentioned above dynamic failure shows frequency dependency. In any way no drastic failure occurred in this experiments. In order to compare above dynamic failure patterns with static ones mentioned before, Fig.6 is quoted from Ref.2. As seen in Fig.6 the depth of sliding surface of the model of same materials and cross section as those of this paper is considerably larger and sliding soil mass is bigger beyond comparison in the cases of static failure. Horizontal component of gravity acceleration in the static failure stated in Ref.2 is 603~617(gal). To generate same amount of sliding mass as in Fig.6 in dynamic loading will need several times of above value for base acceleration. It may be said that failure pattern in static loading differs from the one in dynamic loading and the difference originates in the duration of loading.

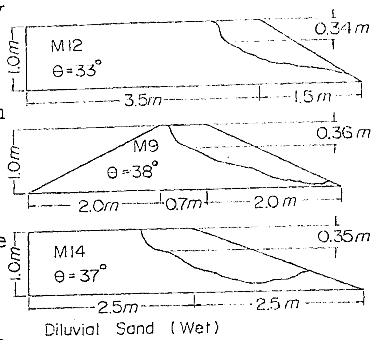

Fig. 6 Typical Shape of Static Failure

NUMERICAL SIMULATIONS OF DYNAMIC FAILURE TESTS

Dynamic Constants In advance of simulations, dynamic torsional shearing tests were carried on the specimens of which average density and water content were arranged to be equal to those of the models under such low confining pressures as in the models, resulting in the following hyperbolic formulations,

$$G = 950\frac{(2.17-e)^2}{1+e}(\sigma'_m)^{0.525}\frac{1}{1+\gamma/2.69\times10^{-4}},\quad h = 0.14\frac{\gamma}{\gamma+2.69\times10^{-4}} \tag{1}$$

where G, e, σ'_m and h are shearing modulus, void ratio, effective mean principal stress and damping constant respectively. Rayleigh type damping with above h was used in the following calculations, as

$$\{c\} = 1.4\,h\,\omega_1\{m\} + 0.6(h/\omega_1)\{k\} \tag{2}$$

where $\{m\}$, $\{k\}$, and $\{c\}$ are the matrices of mass, stiffness and damping of the element respectively and ω_1 is the first natural frequency of a model.
Equivalent Linear Dynamic Analysis Above resonant exciting tests and dynamic failure tests of 5, 15 and 25(Hz) in frequencies of base motion were simulated

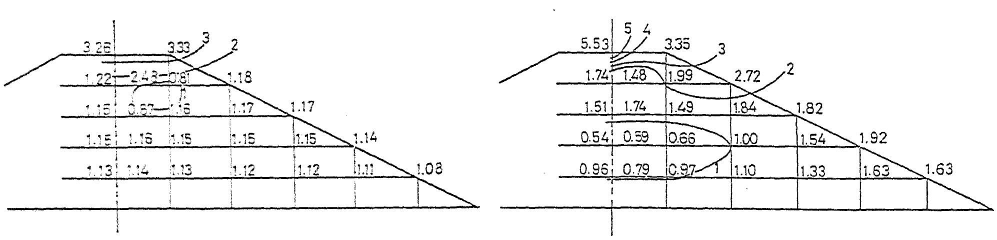

(a) Frequency:5(Hz), Base Acc.:403(gal) (b) Frequency:25(Hz), Base Acc.:351(gal)
Fig. 7 Contours of Magnification of Calculated Response Accelerations in Failure

first with the equivalent linear dynamic analysis. Simulated resonant curves of four intensities of base acceleration agree fairly well with those of experiments in first and second resonant frequencies, in shapes and values of resonant curve and in distributions of amplification of response acceleration. Fig.7 shows the simulated contours of magnification of horizontal response acceleration in failure tests of 5 and 25(Hz) in frequency of base motion. Comparing Fig.7 with Fig.5 it may be seen that both shapes of contour are similar each other. Besides the value of calculated response acceleration was 1330(gal) in case of 5(Hz) and was 1560 (gal) in case of 25(Hz). These are nearly constant though a little larger than those obtained in the experiments. In any way it may be said that the equivalent linear dynamic analysis simulates fairly well above experiments as a whole.

Non-Linear Dynamic Analysis Above mentioned failure tests with 3 sorts of frequency were simulated also by non-linear dynamic analysis where the joint elements of yielding criteria as shown in Fig.8 were inserted into every boundary

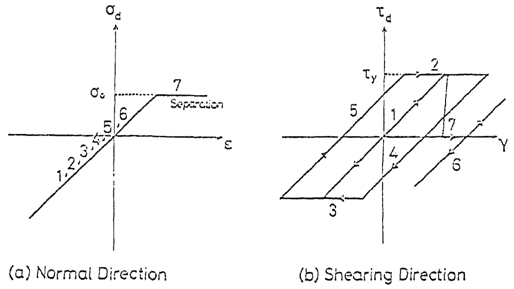

1 : Linear State before Yielding
2 : Strain Increment State in Yielding Domain
3 : Opposite of State 2
4 : Elastic Rebound from Yield State
5 : Opposite of State 4
6 : Virgin Linear State from the Origin of Residual Strain after Separation State 7
7 : Separation State

Fig. 8 Constitutive Relationships of the Joint Element

of all finite elements. The strength parameters c and ϕ used in the criteria are 12.7(grf/cm^2) and 36° respectively which were obtained from usual tri-axial compression tests. The values of spring constants k_s and k_n of every joint element were given to be 1000(kgf/cm^2) that were 20~100 times larger than the stiffness of finite elements so as to make the first natural frequency of every numerical model coincide with the one of the case without joint element. Initial stresses due to gravity were estimated with average elastic constants of $E = 50.5(kgf/cm^2)$ and $\nu = 0.3$ obtained from elastic wave velocities of models. Dynamic moduli and damping constants finally converged in above steady state solution with equivalent linear analysis were applied and fixed in the finite elements in each case. So that, non-linear property was taken into account only in joint elements. In non-linear analysis the load transfer method was applied at every discrete time step Δt taken to be 5×10^{-5}(sec).

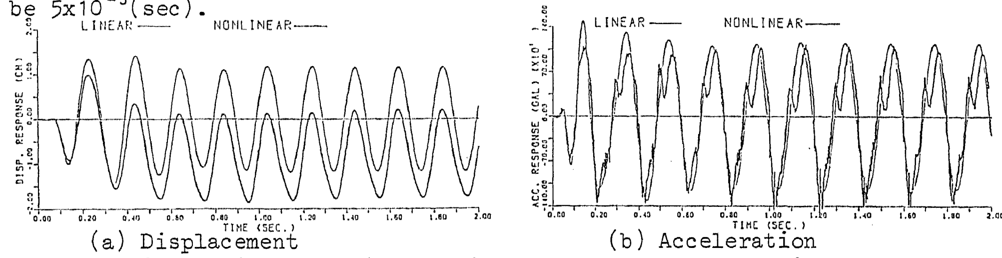

(a) Displacement (b) Acceleration

Fig. 9 Time Histories of Displacement and Acceleration

Results Calculated time histories of displacement and acceleration on the top point of a model in case of 5(Hz) are shown in Fig.9 for an example. From this figures it is seen that the response acceleration in non-linear case is nearly equal to the one in the equivalent linear case though the permanent deformation is generated. Simulated deformations in failure are shown in Fig.10. In case of 5 (Hz) top layer only deformed largely while lower portion remains the original form. In case of 25(Hz) permanent deformation of top layer is not so remarkable but lower part is deformed to the extent of a third part of the height. These states just agree with before mentioned experimental results. It is very interesting to compare above simulated dynamic failure patterns with static ones as done in the experiments. Fig.11 quoted from Ref.2 shows developing of discontinuous elements and accompanying deformation in the simulation of a statical failure by tilting tests. Ref.2 says that a drastic failure of soil structure occurs when discontinuous elements due to sliding or separation are connected and form one continuous curve passing space to space and that it appeared when tilting angle θ attained to 38° as shown in Fig.11 which agrees very well with the experimental results. It may be said that static failured zone is deep and large in the simulation too, that is, dynamic failure is different from static one in the numerical simulation too.

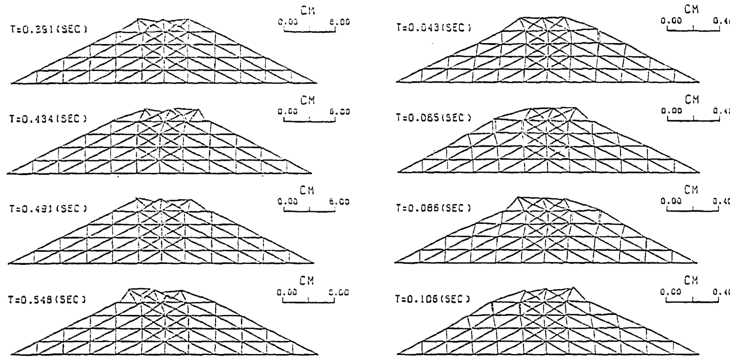

(a) Case of 5(Hz) (b) Case of 25(Hz)

Fig. 10 Simulated Permanent Deformations in Failure

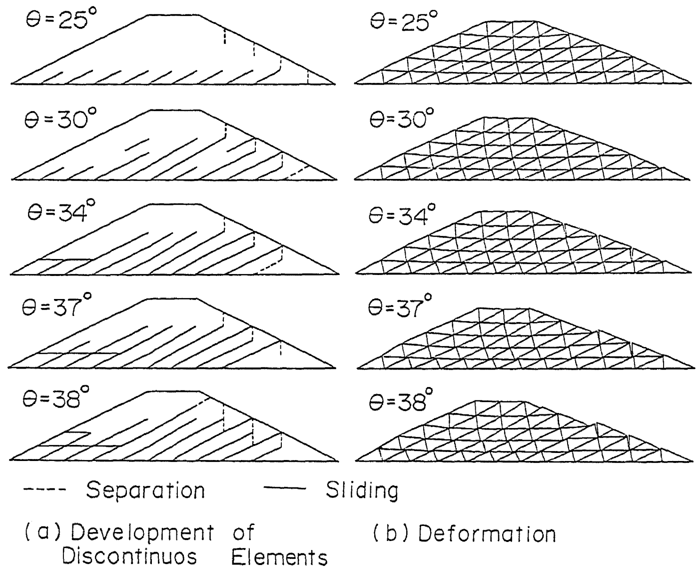

(a) Development of Discontinuos Elements (b) Deformation

Fig. 11 Simulated Static Failure Pattern

CONCLUDING REMARKS

(1) Dynamic failure patterns show a frequency dependency, however, the failure occurs when the values of response accelerations at failured portions attain to a certain constant value independent of frequency.

(2) Equivalent linear analysis simulates fairly well the dynamic failure of soil structures and non-linear one with joint elements can clarify its mechanism.

(3) Dynamic failure is quite different from static one.

REFERENCES

1. Watanabe, H. et al., Evaluation of Earthquake-Induced Sliding in Rockfill Dams, Soils and Foundations, Vol.24, No.3, pp.1-14, Sept., 1984.
2. Watanabe,H. and Saotome, A., Statical Failure Tests by Inclination on Model Slopes of Soils and Numerical Simulation of Them, Proc.JSCE, No.376,pp.31-,1986.